

Removal of Arsenic(III) from Aqueous Solution Using Nano Zerovalent Iron Supported On Sawdust (NZVI/SD)

ABSTRACT

Sawdust supported nano-zerovalent (NZVI/SD) iron was synthesized by treating sawdust with ferrous sulphate followed by reduction with NaBH_4 . The NZVI/SD was characterized by SEM, XRD, FTIR and Chemical method. Adsorption of As(III) by NZVI/SD was investigated and the maximum uptake of As(III) was found at pH value of 7.74 and equilibrium time of 3 hrs. The adsorption isotherm modeling revealed that the equilibrium adsorption data was better fitted with the Langmuir isotherm model compared with the Freundlich Isotherm model. This study revealed that the maximum As(III) ions adsorption capacity was found to be 12.66 mg/g for using NZVI/SD adsorbent. However, the kinetics data were tested by pseudo first order and pseudo second order kinetic models; and it was observed that the adsorption data could be well fitted with pseudo second order kinetics for As(III) adsorption onto NZVI/SD depending on both adsorbate concentration and adsorption sites. The result of this study suggested that NZVI/SD could be developed as a prominent environment friendly adsorbent for the removal of As(III) ions from aqueous systems.

Keywords: Sawdust, nano zerovalent iron, adsorption, isotherm, kinetics.

1. INTRODUCTION

Nowadays environmental pollution with heavy metals is a major environmental concern [1]. These heavy metals are known to be highly toxic even at low concentration. Because, heavy metals are non-biodegradable, and accumulate to certain level which causes different health problems in animals, humans and aquatic organisms [2, 3]. Among different types of heavy metals, arsenic contamination in natural and groundwater has been receiving significant attention. The United States Environmental Protection Agency (US-EPA) and World Health Organization (WHO) have set the maximum allowable concentration (MAC) for As at 0.01 mg/L in drinking water [4]. Materially, arsenic has been introduced into the environment through a combination of natural processes (weathering reactions, biological activities, and volcanic emissions) as well as anthropogenic activities [5]. In addition, Arsenic exists in groundwater predominantly as inorganic arsenite, As(III) (H_3AsO_3 , $\text{H}_2\text{AsO}_3^{1-}$, HAsO_3^{2-}), and arsenate, As(V) (H_3AsO_4 , HAsO_4^{1-} , HAsO_4^{2-}) [6,7,8]. Therefore, it is necessary to eliminate As from the environment in order to prevent its deleterious impact on ecosystem and public health. Besides, greater attention is required for the removal of As(III) from groundwater due to its higher toxicity and mobility compared to the charged As(V) species, which predominate near pH 6-9 [6, 9,10]. So its removal has become a considerable challenge for environmental scientists and engineers [7, 8, 11, 12].

Since arsenic contamination is an extensive problem, many methods have been developed for the removal of arsenic such as adsorption [13,14,15,16], ion exchange [17], reverse osmosis, microbial transformation [18,19], coagulation (co precipitation) [20] and bioremediation [21]. Of these methods, adsorption techniques are relatively simple to conduct and are cost effective. Various materials have already been tested as sorbents such

as: magnetic ion exchange resins, hydrous iron oxide particles, granular ferric hydroxide, activated alumina, sawdust, clay, zeolite, activated carbon and zero valent iron oxide nanoparticles. Attention has recently focused on zero-valent iron (ZVI) for rapid As(III) and As(V) removal in the subsurface environment [9,22]. Therefore, initiatives had been taken to increase the surface area with the view to increase the reactivity of zero-valent iron (ZVI) had been emerged eventually. Its significance to remove varieties of pollutants such as, TCE, PCE [23,24,25,26], carbon tetrachloride [27], heavy metals (e.g., Ni^{2+} , Hg^{2+}), As(III) [28] and organic compounds such as benzoic acid [29]. Furthermore, direct application of NZVI particle in water treatment system may cause fast loss of NZVI particle and lead to iron pollution due to its small particle size. Hence, for the treatment of pollutant it is necessary to load NZVI particle onto an efficient supporting material. In this study, sawdust was more economical and easily available as supporting materials for NZVI. Herein, we have demonstrated that the sawdust supported NZVI particle showed much better As(III) adsorption, while sawdust itself was not an efficient adsorbent for arsenic.

2. MATERIAL AND METHODS

2.1 ADSORBENT AND REAGENTS

Sawdust of *Shorea robusta* commonly known as Salt in Bangladesh was collected from a saw mill at Mirpur-1, Dhaka as principal raw material. It was then washed repeatedly with sufficient amount of demineralized water to remove dust and soluble impurities and dried at 100 °C for 12 hr. It was screened in with a sieves and size of 1.18 mm (oversize), was collected and was preserved in a hermetic plastic bottle. In order to avoid moisture, 2-3 silica gel packets were introduced in the bottle. Chemical analysis of the sawdust were done using standard methods [30] and found that it contained 7.3% extractible materials, 57.6% cellulose and 28.1% lignin. A 1000 ppm arsenious acid (H_3AsO_3 , ACS, ISO, reagent grade, Merck-KgaA, Germany) solution; Ferrous sulphate heptahydrate ($\text{FeSO}_4 \cdot 7\text{H}_2\text{O}$, ACS, reagent grade, Merck-KgaA, Germany); sodium borohydride (NaBH_4 , 99.99%, Merck, Germany) were used as received. Stock solution of As(III) compound was further diluted to desired concentration using deionized water.

2.2 PREPARATION OF THE ADSORBENT

Sawdust supported nanoscale zero valent iron (NZVI) have been synthesized following a literature protocol [31]. The synthesis of NZVI/SD was performed in a three open necks. The dried sawdust (2.0 g) was soaked in N_2 – purged ferrous sulfate solution (30 ml and 1.0 M) and left for three hours. The slurry was diluted by five times using a mixture of ethanol and deionized water (v/v 1:1). NaBH_4 (0.2 M, 100 ml) was then added drop wise (1.0 mL/min) into the slurry at 25 °C temperature under magnetic stirring and N_2 bubbling, which resulted in the rapid formation of fine black solid particles and deposited on sawdust. After 30 minutes of agitation, the sawdust supported NZVI was separated from the mixture by filtration through glass sintered funnel under vacuum. The solid particles thus obtained were washed with acetone (3*20 ml), dried at 60 °C temperature in an oven for 8 h. Finally, the dried powder sample was stored in a desiccator for further use.

2.3 BATCH ADSORPTION EXPERIMENTS

NZVI/ sawdust (10 mg) was added to aqueous solution of As(III) (10 ml, 22 ppm and 35 ppm) in 25 ml conical flasks and the solutions were left out at 25 °C and shaking in an orbital shaker at 180 rpm for 3 hours (equilibrium time). The effect of pH (2.1 to 11.4) on the removal of arsenic(III) was studied with constant adsorbent dosage of 1 g/L, adsorption time of 180 minutes, agitation speed of 180 rpm and metal ion concentration of 20.5 ppm. The

effect of contact time was studied with initial As(III) concentrations of 22 and 37 ppm, pH of 7.74 and a constant adsorbent dosage of 1 gL⁻¹. The effect of initial As(III) ions concentration was studied by varying the initial concentration of As(III) from 18.5 to 44.7 mg L⁻¹, while maintaining the adsorbent dosage of 1 gL⁻¹, contact time of 180 minutes and equilibrium pH of 7.74. The amount of As(III) adsorbed per unit mass of the adsorbent (q) was obtained by using the following equation (Eq. (1)):

$$q = \frac{(C_i - C_e) V}{m} \dots\dots\dots(1)$$

Where C_i and C_e are initial and equilibrium concentrations of the metal ions (g/L), m is dry mass of the adsorbent (g) and V is the volume of the solution (L).

2.4 ANALYSIS THE SAMPLES

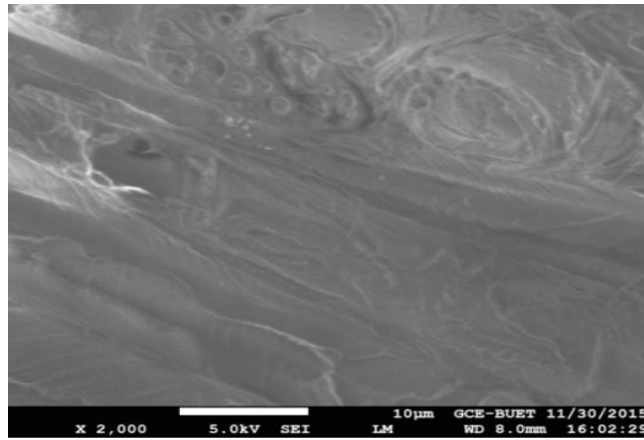
The Adsorbents were characterized using a FTIR 8400S Shimadzu spectrophotometer (Irpstige-21 model, Shimadzu, Japan) in the range of 4000 to 700 cm⁻¹ and 20 scanning rate with a resolution of 4 cm⁻¹. Experiments were carried out using ATR sampling technique. The morphology of the adsorbents were also characterized using a JEOL JSM-7600F Field Emission Scanning Electron Microscope (SEM) coupled with Energy-Dispersive X-ray (EDX) spectroscopy at an accelerating voltage of 5.0/kV and a working distance of 8 mm. For X-ray diffraction analysis, an X-ray Diffractometer (XRD) was used (Ultima IV, Rigaku Corporation, Japan) at 40 kV and 40 mA for a scan range of 2θ from 20° to 100°. The pH measurements were performed using a pH meter (Hanna instruments, HI 2211-02, Hanna, Romania). An orbital Shaker (SSL1, Stuart UK) was used for the batch adsorption experiments. After the adsorption process, the metal solution was filtered through Whatman 41 filter paper. The residual As(III) was analyzed using atomic absorption spectroscopy (AA240, Varian, Australia) at the Analytical Chemistry Laboratory, Chemistry Division, Atomic Energy Centre, Dhaka, Bangladesh.

3. RESULTS AND DISCUSSION

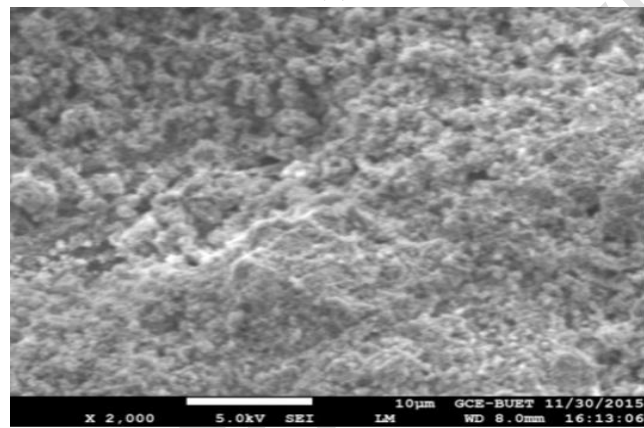
3.1 CHARACTERIZATION OF NZVI/SD

3.1.1 SCANNING ELECTRON MICROSCOPE

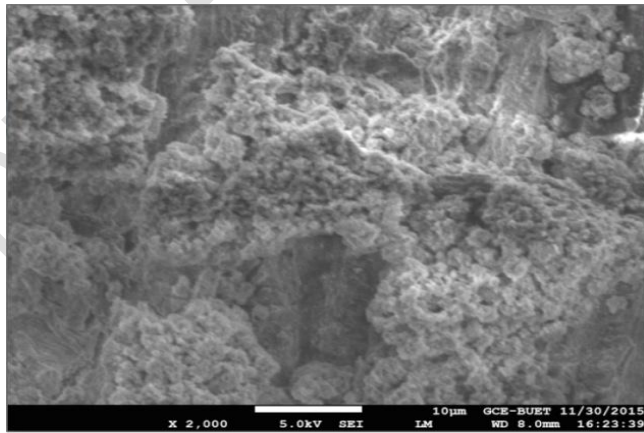
The cell wall of sawdust mainly consists of dry matter (96.93%). The proximate composition of wood sawdust is 7.3% extractible materials, 57.6% cellulose and 28.1% lignin. Cellulose,



(a)



(b)



(c)

Fig. 1. Scanning electron microscope for (a) raw sawdust, (b) freshly prepared NZVI/SD and (c) finally after used for As(III) ions adsorption study.

hemicellulose and lignin are the main components of acid detergent fiber. All those compounds are active ion exchange compound [30]. The surface structure of wood sawdust was analyzed using a scanning electron microscope (SEM) for raw sawdust (Fig. 1(a)), freshly prepared NZVI/SD (Fig. 1(b)) and finally after used for As(III) ions adsorption study (Fig. 1(C)). The SEM micrograph of the freshly prepared NZVI/SD (Fig. 1(b)), revealed that the surface of the sawdust appeared to be quite rough as seen at 2000X magnification. This Figure also clearly showed that non-uniform particle size with the presence of pores on the sawdust surface. It revealed that the ZVIN saw dust samples were spherical in shape and polydispersed in nature with different sizes. Comparing the size of the particles with the scale of the Fig. 1(a), it has been confirmed that the size of the iron particles on the surface of NZVI/SD was ranging from 10 to 80 nm and almost uniform sized particles were observed. However, the SEM image of saturated NZVI/SD was shown in Fig. 1(c). From this Fig. 1(c), it was suggested that after adsorption of As(III) ions, the surface of NZVI was more even than fresh NZVI/SD and the particles were almost uniformly dispersed in the saturated NZVI/SD. From the SEM images, it was also observed that the adsorbent revealed a porous nature, considerable number of heterogeneous pores and particle aggregation of various shapes and sizes. Generally, the porous nature of the adsorbents revealed their suitability for adsorption of As (III) from aqueous solution [34].

3.1.2 FOURIER-TRANSFORM INFRARED (FTIR) SPECTROSCOPY

The metal adsorption capacity is influenced strongly by the surface structures of carbon-oxygen (functional groups) and surface behavior of carbon [16]. Functional groups in wood sawdust were determined using Fourier-transform infrared (FTIR) spectroscopy (Fig. (2)).

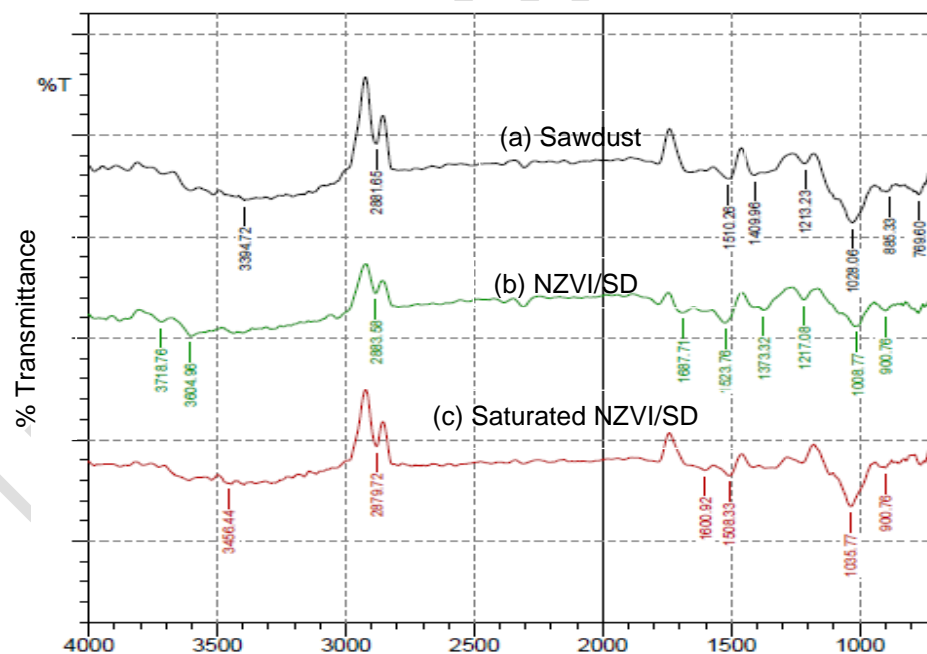


Fig. 2. FTIR spectrums for (a) raw sawdust, (b) freshly prepared NZVI/SD and (c) finally after used for As(III) ions adsorption study.

The untreated wood sawdust FTIR spectrum showed eight major intense bands at 769.6 cm^{-1} , 885.33 cm^{-1} , 1028.06 cm^{-1} , 1213.23 cm^{-1} , 1409.96 cm^{-1} , 1510.26 cm^{-1} , 2881.65 cm^{-1} , and 3394.72 cm^{-1} , whereas treated NZVI sawdust showed nine bands at 900.76 cm^{-1} , 1008.77 cm^{-1} , 1217.08 cm^{-1} , 1373.32 cm^{-1} , 1523.76 cm^{-1} , 1687.71 cm^{-1} , 2883.58 cm^{-1} , 3604.96 cm^{-1} and 3718.76 cm^{-1} and As(III) ions adsorbed saturated NZVI/SD showed six bands at 900.76 cm^{-1} , 1035.77 cm^{-1} , 1508.33 cm^{-1} , 1600.92 cm^{-1} , 2879.72 cm^{-1} , and 3456.44 cm^{-1} respectively. The FTIR spectrum of sawdust shows a broad band, at 3456 cm^{-1} , is attributed to the hydrogen bonded -OH stretching of phenol (-OH) groups can undergo protonation reactions [32]. The band appearing at (2879 to 2881.65 cm^{-1}) corresponds to CH stretching vibrations from $-\text{CH}_2$. The presence of a band at around 1600 cm^{-1} may be due to amide (N-H) groups in sawdust. A band appearing at 1053 is due to C-O in cellulose, ether, carboxylic acids and other natural compounds present [33]. The FTIR(ATR) spectra of NZVI/SD is similar to that of the spectrum of sawdust because of Fe, which a metal was used to modify the sawdust and there was no change in the cellulose of the sawdust. If Fe was present in its oxide form then there would have been new peaks in the FTIR spectra of NZVI/SD.

3.1.3 X-RAY DIFFRACTOGRAMS (XRD)

The X-ray diffractograms of raw sawdust and sawdust supported Nano-zerovalent (NZVI/SD) iron were shown in Fig. 3. This analysis was carried out to evaluate the crystalline nature and size of sawdust supported nano-zerovalent (NZVI/SD) iron.

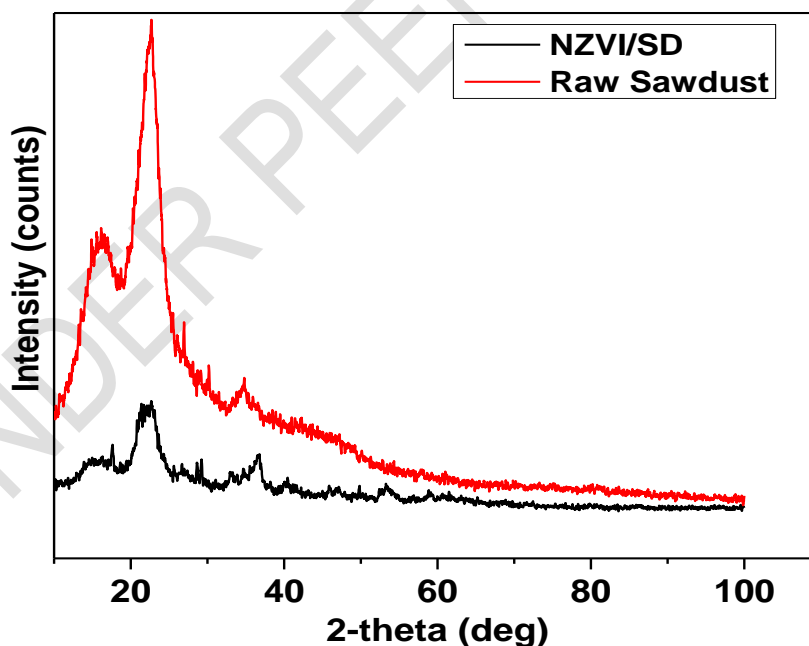


Fig. 3. XRD for Sawdust and NZVI/SD

Fig. 3 reveals that the diffraction peaks were located at 30.1, 35.5, 41.6, 53.6 and 57.0 are evident of XRD pattern of synthesized iron nanoparticles [35]. It also reveals that the iron present in the sample is mainly in its zero-valent state and all zero-valent irons are in a single phase cubic closed packed structure and amorphous in nature [36]. However, two additional peaks around 16° and 22° are evident in Fig. (3). These two peaks could be attributed to raw sawdust, due to presence of carbon in the sawdust sample. It is also evident from the figure that the intensities of these two peaks were decreased markedly, demonstrating partial carbon degradation of NZVI/SD sample. This may be due to the fact that the porous structure of sawdust decreased after iron deposition on its surface. Hence the crystalline phases of sawdust may have been reduced after iron deposition [37]. Crystallite Size of ZVIN is calculated from Scherrer's formula, given below:

$$D = \frac{0.9\lambda}{\beta \cos \theta} \dots \dots \dots (2)$$

Where, D is the crystallite size in Å, λ the wavelength of Cu K_{α} radiation, i.e., 1.54 Å, β the full width at half maximum (FWHM), and θ is the angle obtained from 2θ corresponding to maximum peak intensity. The crystalline dimension of the Fe⁰ particles was found to be 4.96 nm.

Iron content present in the synthesized NZVI/SD was determined by a chemical method. In this case, 0.05g of adsorbent was mixed with 15ml of 7M HCl, followed by shaking at 25°C for 2 hours. The supernatant was collected by filtration and analyzed on an atomic absorption spectrophotometer (Model: PerkinElmer Analyst 800) [38]. Fe content was found to be 38.8 mg of Fe per gram of adsorbent.

3.2. ARSENIC(III) IONS REMOVAL

3.2.1 EFFECT OF pH

The pH- dependent behaviour of the adsorption of As(III) on the NZVI/SD is shown in the Fig (4).The variation of adsorption capacity from 3 mg/g to 8.32 mg/g was observed in the pH range 2.2-11.07. The pH- dependent behaviour can be illustrated in terms of the existence of the different forms of As(III), surface complexation and electrostatic interactions. At pH< 9.1 As(III) exist as neutral compound(H₃AsO₃) while at 9.1 < pH < 12.1, it exists as anions H₂AsO₃⁻ [32,39].From the figure it is apparent that the adsorption capacity was increased from 3 to 8.32 in the pH range 2.0 to 8 because of the existence of neutral compound, H₃AsO₃ in this pH range and this result implies that adsorption is controlled by surface complexation process. Moreover, further increase of basicity reduced the adsorption capacity due to the presence of anions H₂AsO₃⁻, which confirms that at pH > 8, the adsorption of As(III) on NZVI/SD depends on electrostatic interactions. The similar result could be obtained by the literature of [13, 27, 33].

3.2.2 EFFECT OF TIME

To find out the effect of agitation time on As(III) ions adsorption onto NZVI/SD in, this study was conducted for an adsorption dose of 10 mg in 10 mL of 22 ppm and 37 ppm of As(III) solutions for the agitation time of 5, 10, 20, 30, 40, 60, 120, 180 and 240 minutes respectively. The study revealed that As(III) ions adsorption capacity of NZVI/SD adsorbent was increased rapidly for the first 40 minutes, and then increase slowly with increasing of agitation time (Fig. 5). For instance, the optimum As(III) ions adsorption capacity of NZVI/SD for the initial 22 ppm As(III) solution was observed for the agitation time of 40 min and then very slowly increased with the increase of agitation time. A same trend was observed for the

37 ppm As(III) solution, which showed that the optimum As(III) ions adsorption capacity of NZVI/SD adsorbent was obtained around 60 minutes. Furthermore, there was significant difference of adsorption among the obtained data for 120 min and 180 min. As a consequence, 60 min contact time was chosen as an optimum time in each experiment.

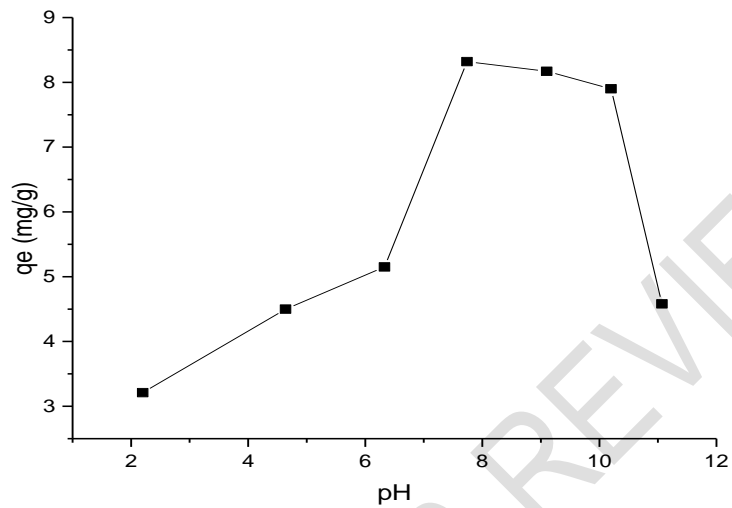


Fig. 4. Effect of pH on As(III) ions adsorption by NZVI supported on sawdust

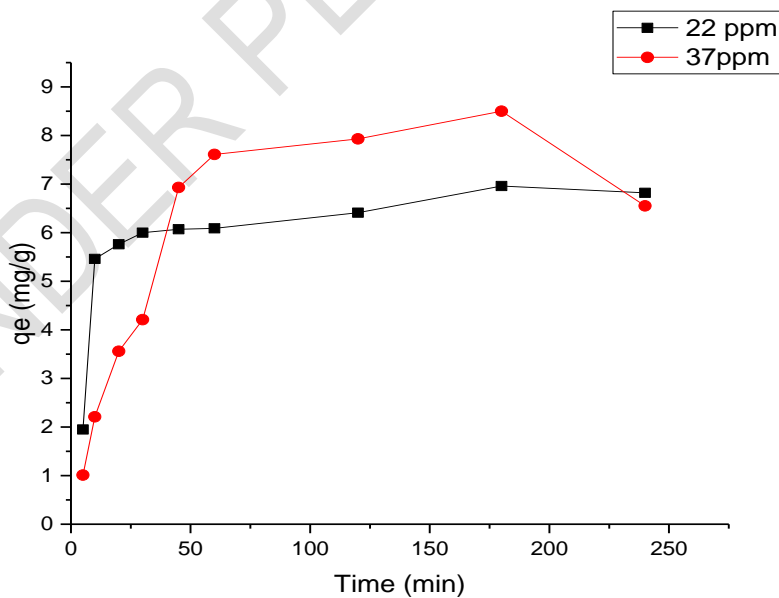


Fig. 5. Effect of contact time on As(III) ions adsorption using NZVI/SD adsorbent

3.3. ADSORPTION ISOTHERM

In order to explain the nature of interaction between adsorbate and adsorbent, two adsorption isotherm models namely Langmuir and Freundlich isotherm models were tested. The Langmuir adsorption isotherm model is based on the assumption that the adsorption process proceeds through monolayer homogeneous adsorption, while, Freundlich isotherm model supports multilayer heterogeneous adsorption process [39]. The linearized form of Langmuir and Freundlich isotherm models are given following Eq. (3) and Eq. (4).

$$\frac{C_e}{q_e} = \frac{C_e}{q_{\max}} + \frac{1}{q_{\max} K_L} \dots\dots\dots(3)$$

$$\log q_e = \log K_F + \frac{1}{n} \log C_e \dots\dots\dots(4)$$

Where, q_e is the adsorption capacity of adsorbent at equilibrium (mg/g), C_e is the concentration of adsorbent at equilibrium (mg/L), q_{\max} is the maximum monolayer adsorption capacity (mg/g), K_L is the Langmuir isotherm constant(L/mg)which represents the affinity between the solute and adsorbent, K_F is Freundlich constant related to adsorption capacity of the adsorbent, n is a constant of Freundlich isotherm which gives the probability of adsorption process and $1/n$ is the adsorption intensity.

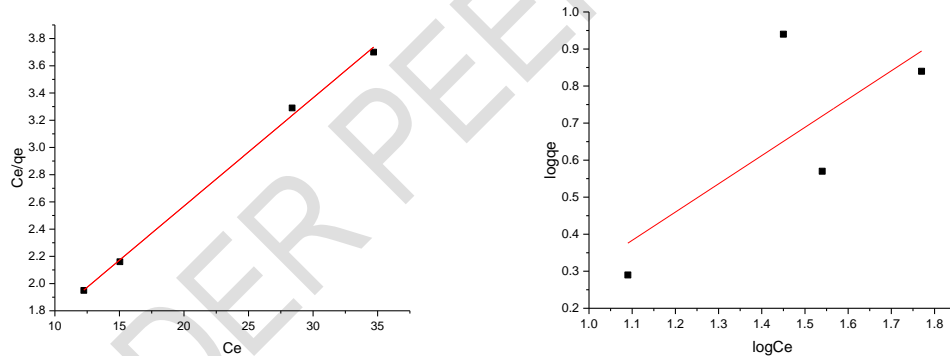


Fig. 6. Langmuir Isotherm (Left) and Freundlich Isotherm (Right) for adsorption of As(III) on NZVI supported on sawdust.

The value of correlation coefficient r^2 for Langmuir isotherm was 0.997 while that for Freundlich isotherm was 0.554. It was concluded that the adsorption process fitted with Langmuir adsorption process that indicates the adsorption of As(III) on NZVI/SD is monolayer homogeneous adsorption [42]. The maximum monolayer adsorption capacity was found to be 12.66 mg/g obtained from the Langmuir isotherm model. The isotherm parameters are listed in the Table 1. A comparison is made between NZVI/SD and some adsorbent materials for the removal on As(III) that are listed in Table 2.

Table 1. Adsorption Isotherm Parameters for the Adsorption of As(III) on NZVI/Sawdust.

| Adsorbent | Langmuir Isotherm Model | | | Freundlich Isotherm model | | |
|-----------------|-------------------------|-------|-------|---------------------------|-------|-------|
| | q_{max} | K_L | R^2 | n | K_F | R^2 |
| NZVI on sawdust | 12.66 | 0.081 | 0.997 | 1.31 | 0.35 | 0.554 |

Table 2. Comparison of As(III) adsorption capacity with some adsorbent materials in the references

| Adsorbent | Adsorption Capacity(mg/g) | Referrance |
|---|---------------------------|------------|
| Sawdust Carbon | 1.716 | 41 |
| Nanozervalent Iron nanoparticle | 3.5 | 42 |
| Magnetic nanoparticles | 3.7 | 43 |
| Iron-containing ordered mesoporous carbon | 9.3 | 20 |
| Nanozerovalent iron supported on Sawdust | 12.66 | This Paper |

R_L is a dimensionless constant called separation factor or equilibrium factor, which is expressed by the following equation [40]

$$R_L = \frac{1}{1 + K_L C_i} \dots \dots \dots (5)$$

Where, C_i is the initial concentration of the adsorbate (mg/L), K_L is the Langmuir constant. The value of R_L is from 0 to greater than 1. The Langmuir isotherm is irreversible, linear, unfaourable, favourable at $R_L = 0$, $R_L = 1$, $R_L > 1$ and $0 < R_L < 1$ respectively. R_L was found to be from 0.22 to 0.40 indicating that the adsorption of As(III) on NZVI on sawdust is favourable in the range of 18.5 to 44.7 ppm concentration (Table 3).

Table 3. Separation Factor values for the adsorption of As(III) on NZVI/Sawdust.

| Metal | Initial concentration(ppm) | R_L Value |
|---------|----------------------------|-------------|
| As(III) | 18.5 | 0.40 |
| | 22 | 0.36 |
| | 37 | 0.25 |
| | 44.7 | 0.22 |

3.4. ADSORPTION KINETICS

Pseudo first order and second order kinetics model were tested to describe the adsorption mechanism of As(III) on NZVI/Sawdust. The linearized form of pseudo first order and second order kinetics equations are given below

$$\ln(q_e - q_t) = \ln q_e - K_1 t \dots \dots \dots (6)$$

$$\frac{t}{q_t} = \frac{1}{K_2 q_e^2} + \frac{t}{q_e} \dots \dots \dots (7)$$

Where q_e is the adsorption capacity of adsorbent at equilibrium, q_t is the adsorption capacity of adsorbent at time t , t is time (min), K_1 is the rate constant for pseudo first order reaction, min^{-1} and K_2 is the rate constant for pseudo second order reaction $\text{g mg}^{-1}\text{min}^{-1}$. Variation of adsorption capacity of the adsorbent with time is shown in Fig. (7). From the figure it was clear that the adsorption process reached equilibrium at 3 hours.

The plot of $\ln(q_e - q_t)$ vs t is shown in Fig. (7) and it is lucid that the experimental data did not fit well with pseudo first order kinetics model, while it fitted well with the pseudo second order kinetics (right). Thus the adsorption of As(III) on sawdust supported NZVI depends on both the As(III) concentration and available active sites of the adsorbent. With the increase of initial concentration of As(III) solution rate constant of pseudo second order kinetics model decreased from 0.019 to 0.0024 (Fig 7). This also explains that the adsorption process depends on As(III) concentration. Similar phenomenon of adsorption kinetics on As(III) adsorption was reported previously [33,41]. Different kinetic parameters that were obtained from the graphs are listed in the Fig 7.

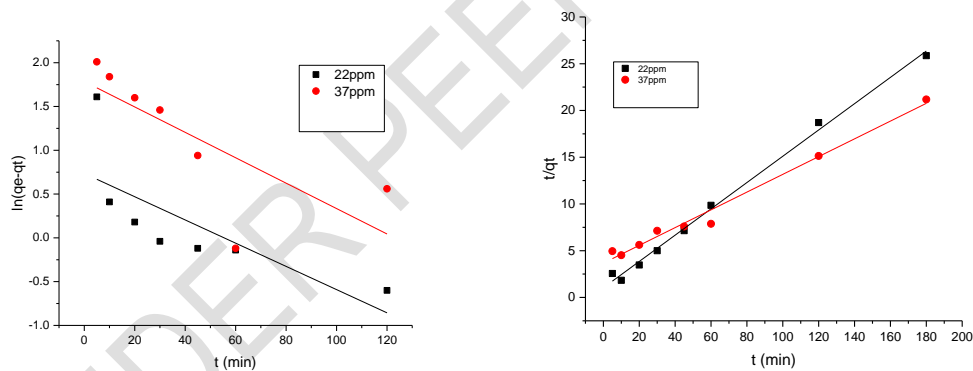


Fig. 7. As(III) ions adsorption study using on NZVI supported on sawdust for (a) pseudo first order kinetics and (b) pseudo second order kinetics

4. CONCLUSION

In this study, NZVI/SD was successfully synthesized by impregnating sawdust with ferrous sulphate followed by chemical reduction of Fe(II) to Fe(0). Adsorption performance of as prepared adsorbent for the removal of As(III) from aqueous solution was investigated. It was found that equilibrium time and optimum pH were 3 hours and 7.74 respectively for this adsorption process. SEM results revealed that NZVI appear as a spherical particle with a particle size in the range 10-80 nm. The uptake of As(III) by NZVI/SD is a homogeneous adsorption process as the adsorption process followed Langmuir Isotherm model. Kinetics of this adsorption process can be better explained by pseudo second order

model. This model indicates both adsorbate and adsorbent which influence the adsorption of As (III) on NZVI/SD. Therefore, the present study suggests that NZVI/SD is a promising and effective material for the removal of As(III) from aqueous solution.

REFERENCES

- [1] Ferguson J F, Gavis, J. A review of the arsenic cycle in natural waters. *Water Res.* 1972; 6:1259-1274.
- [2] Bajpai S, Chaudhary M. Removal of arsenic from groundwater by manganese dioxide-coated sand. *J. Environ. Eng.* 1999;125:782-784.
- [3] Tseng WP, Chu HM, How SW, Fong JM, Lin, CS, Yeh, SJ. Prevalence of skin cancer in an endemic area of chronic arsenism in Taiwan. *J. Natl. Cancer Inst.* 1968; 40:453-463.
- [4] CHEN CW, CHEN CJ. Integrated quantitative cancer risk assessment of inorganic arsenic. *Proceedings of Symposium on Health Risk Assessment on Environmental, Occupational and Life Style Hazards, December 20-22, (1988), Institute of Biomedical Science, Academia Sinica, Taipei.* 1991; 65-80.
- [5] Goldberg S, Johnston CT. Mechanisms of arsenic adsorption on amorphous oxides evaluated using macroscopic measurements, vibrational spectroscopy, and surface complexation modeling. *J. Colloid Interface Sci.* 2001; 234:204-216.
- [6] Clifford, DA, Zang Z. Arsenic chemistry and speciation. *Proceedings of the 1993 Water Quality Technology Conference, AWWA, Denver, CO, April, 1994.*
- [7] Smith A.H., Lingas E.O., Rahman M., Contamination of drinking-water by arsenic in Bangladesh: a public health emergency, *Bulletin of the World Health Organization.* 2000;78(9):1093–1103.
- [8] Berg M. Arsenic contamination of groundwater and drinking water in Vietnam: a human health threat, *Environ. Sci. Technol.* 2001; 35(13):2621–2626.
- [9] Manning BA, Hunt M, Amrhein C, Yarmoff JA. Arsenic(III) and arsenic(V) reactions with zerovalent iron corrosion products. *Environ. Sci. Technol.* 2002; 36:5455-5461.
- [10] Gulens J, Champ DR, Jackson RE. In *Chemistry of Water Supply Treatment and Distribution*; Rubia AJ, Ed.; Ann Arbor Science Publishers: Ann Arbor, MI, 1973.
- [11] Bagla P, Kaiser J. India's spreading health crisis draws global arsenic experts, *Science (New York, NY)* 1996; 274: 5285.
- [12] Souter PF, Cruickshank GD, Tankerville MZ, Keswick BH, Ellis BD, Langworthy DE et al., Evaluation of a new water treatment for point-of-use house-hold applications to remove microorganisms and arsenic from drinking water, *J Water Health.* 2003 ;1(2):73-84
- [13] Zhu H, Jia Y, Wu X, Wang H. Removal of arsenic from water by supported nano zero-valent iron on activated carbon, *J Hazard Mater.* 2009;172(2-3)1591–1596.
- [14] Sperlich A, Werner A, Genz A, Amy G, Worch E, Jekel M. Breakthrough behavior of granular ferric hydroxide (GFH) fixed-bed adsorption filters: modeling and experimental approaches, *Water Res.* 2005;39(6):1190–1198.
- [15] Zhang QL, Lin YC, Chen X, Gao NY. A method for preparing ferric activated carbon composites adsorbents to remove arsenic from drinking water, *J Hazard Mater.* 2007;148(3):671–678.
- [16] Reddy KJ, McDonald KJ, King H. A novel arsenic removal process for water using cupric oxide nanoparticles, *J Colloid Interface Sci.* 2013; 397: 96–102
- [17] Kim J, Benjamin MM. Modeling a novel ion exchange process for arsenic and nitrate removal, *Water Res* 2004; 38(8): 2053–2062.
- [18] Akin I, Arslan G, Tor A, Cengeloglu Y, Ersoz M. Removal of arsenate [As(V)] and arsenite [As(III)] from water by SWHR and BW-30 reverse osmosis, *Desalination.* 2011;281: 88–92.
- [19] Ning RY. Arsenic removal by reverse osmosis, *Desalination.* 2002; 143 (3):237–241.

- [20] Zouboulis A, Katsoyiannis I. Removal of arsenates from contaminated water by coagulation-direct filtration. *Sep Purif Technol.* 2002; 37(12):2859–2873.
- [21] E.O. Omoregie, et al., Arsenic bioremediation by biogenic iron oxides and sulfides, *Applied and Environmental Microbiology* 79 (14) (2013).
- [22] Su C, Puls RW. Arsenate and arsenite removal by zerovalent iron: effects of phosphate, silicate, carbonate, borate, sulfate, chromate, molybdate, and nitrate, relative to chloride. *Environ. Sci. Technol.* 2001; 35: 4562-4568.
- [23] Wang CB, Zhang W. Synthesizing nanoscale iron particles for rapid and complete dechlorination of TCE and PCBs. *Environ. Sci. Technol.* 1997; 31:2154-2156.
- [24] Lien HL, Zhang, W. Transformation of chlorinated methanes by nanoscale iron particles. *J. Environ. Eng.* 1999; 125:1042-1047.
- [25] Schrick B, Blough JL, Jones AD, Mallouk TE. Hydrodechlorination of trichloroethylene to hydrocarbons using bimetallic nickel-iron nanoparticles. *Chem. Mater.* 2002; 14: 5140-5147.
- [26] Lowry GV, Johnson KM. Congener-specific dechlorination of dissolved PCBs by microscale and nanoscale zerovalent iron in a water/methanol solution. *Environ. Sci. Technol.* 2004; 38:5208-5216.
- [27] Kanel SR, Manning B, Charlet L, Choi H. Removal of arsenic- (III) from groundwater by nano scale zero-valent iron. *Environ. Sci. Technol.* 2005; 39: 1291-1298.
- [28] Joo SH, Feitz AJ, Sedlak DL, Waite, T. D. Quantification of the oxidizing capacity of nanoparticulate zerovalent iron. *Environ. Sci. Tech.* 2005; 39:1263-1268.
- [29] Izyan K, Razak W, Mahmud S, Othman S, Affendy H, Roziela HA, Andy RMM. Chemical Changes in 15 Year-old Cultivated Acacia Hybrid Oil-Heat Treated at 180, 220 and 220°C, *Intl. J. Chem.* 2010; 2: 97-107.
- [30] Wang Y, Gao BY, Yue WW, Yue QY. Preparation and utilization of wheat straw anionic sorbent for the removal of nitrate from aqueous solution, *J Environ Sci (China)*. 2007; 19(11):1305-10.
- [31] Huijie Z, Yongfeng J, Xing W, He W. Removal of arsenic from water by supported nano zero-valent iron on activated carbon. *J. Hazard. Mater.* 2009; 172(2–3):1591–1596.
- [32] Ringbom. A. *Complexation in Analytical Chemistry*. Interscience-Wiley, New York. NY. 1963.
- [33] Chandra V, Park J, Chun Y, Lee JW, Hwang IC, Kim KS. *Water-Dispersible Magnetite-Reduced Graphene Oxide Composites for Arsenic Removal*. *ACS Nano*. 2010; 4(7):3979–3986.
- [34] Patricia I, Clara B, Marcos G (), “The adsorption of chromium (VI) from industrial” wastewater by acid and base-activated lignocellulosic residues,” *J. Hazard. Mater.* 2007; 144(1–2):400–405.
- [35] Sravanthi V, Ayodhya D, Swamy PY. Green synthesis, characterization of biomaterial-supported zero-valent iron nanoparticles for contaminated water treatment. *J Anal Sci Technol.* 2018; 9:3.
- [36] Mohan D, Pittman CU. Arsenic removal from water/wastewater using adsorbents—a critical review, *J Hazard Mater.* 2007; 142(1-2):1-53.
- [37] Ali RR, Samadi MT, Roghayeh N. Hexavalent Chromium Removal from Aqueous Solutions by Adsorption onto Synthetic Nano Size ZeroValent Iron (nZVI). *World Acad. Sci. Eng. Technol.* 2011; 5(4171): 80–83.
- [38] Gu Z.M.; Fang, J.; Deng. B.L. Preparation and Evaluation of GAC-Based Iron-Containing Adsorbents for Arsenic Removal. *Environ. Sci. Technol.* 2005; 39(10):3833–3843,
- [39] Mohan D. Pittman CU. Arsenic removal from water/wastewater using adsorbents—a critical review, *J Hazard Mater.* (2007); 142(1-2):1-53.
- [39]. Hall KR, Eagleton LC, Acrivos A, Vermeulen T. Pore- and solid-diffusion kinetics in fixed-bed adsorption under constant-pattern conditions. *Ind Eng Chem Fundam* 1966; 5(2):212–223

- [40]. McKay G, Otterburn MS, Sweeney AG. The removal of colour from effluent using various adsorbents. III. Silica: rate processes. *Water Res* 1980;14(1):15–20.
- [41] Luo X, Wang C, Luo S, Dong R, Tu X, Zeng G. Adsorption of As (III) and As (V) from water using magnetite Fe₃O₄-reduced graphite oxide–MnO₂ nanocomposites. *Chem Eng J*, 2012;187:45–52.
- [42] Nagarnaik PB, Bhole AG, Natarajan GS. Arsenic(III) removal by adsorption on sawdust carbon. *Int J Environ Pollut Res*.2003;19(2):177.
- [43] Gu Z, Deng B, Yang J. Synthesis and evaluation of iron-containing ordered mesoporous carbon (FeOMC) for arsenic adsorption. *Microporous Mesoporous Mater*, 2007;102(1-3):265–273.

UNDER PEER REVIEW